Lecture 8: Formation of the Solar Wind

Aims, learning outcomes, and overview

Aim: To describe the theory for the origin of the solar wind, and to introduce some of the observational and theoretical characteristics of the wind.

Learning outcomes: At the end of this lecture, students are expected to:

- understand why hydrostatic models of the solar atmosphere are incompatible with interstellar gas pressures;
- be able to derive the equation describing Parker's original steady unmagnetised wind solution;
- be able to explain why a unique solution to this equation applies to the solar wind;
- be aware of the close analogy between Parker's solution and fluid flow in nozzles and rocket exhausts;
- understand the origin of the Parker spiral describing the shape of magnetic field lines in the solar wind;
- understand how Parker's theory may be modified to incorporate a magnetic field in a self-consistent way;
- appreciate the qualitative features of equatorial magnetised wind solutions;
- understand the role of the solar wind magnetic field in angular momentum transport;
- be aware of the properties of the fast and slow components to the observed solar wind, and their origin at the Sun.

Overview: The outer atmosphere of the Sun is continously expanding due to the pressure difference between the hot corona and the cool interstellar medium. This expansion is called the *solar wind*. In this lecture an outline of E.N. Parker's original theory for the solar wind is given, followed by the modification of the theory to include the effects of the magnetic field. The wind is also linked to the velocity filtration model for the corona. A number of recent developments are also discussed, including the observational identification of fast and slow solar wind components.

8.1 Introduction

A theory predicting the existence of the solar wind was given by E.N. Parker in 1958, although there were earlier observational suggestions of the existence of the wind, based on the study of geomagnetic storms and other activity on Earth that could be correlated with solar flares and other activity (sometimes called solar-terrestrial relations) and on the behaviour of the tails of comets. In the first half of this century, "solar corpuscular radiation" was commonly invoked to explain aurorae and geomagnetic activity, although the radiation was assumed to be associated with solar activity and thought to be transient rather than continuous. In the 1950s, Biermann argued that the anti-sunward orientation of the ionised tails of comets was produced by an interplanetary background of ions flowing continuously and radially from the Sun. However, Biermann's model required large velocities and an uncomfortably large density of ions, and had no theoretical basis.

By the 1950s it was well-established that the solar corona is at a temperature of several million degrees. At this temperature, the thermal conductivity of the gas is very high (about twenty times that of copper at room temperature!). The consequences of the high coronal conductivity were explored by Chapman in 1957. The conductivity is dominated by the electron conductivity, which may be written

$$\mathbf{F} = -\kappa_0 T^{5/2} \nabla T, \tag{8.1}$$

where $\kappa_0 \approx 1.8 \times 10^{-11}\,\mathrm{W\,m^{-1}\,K^{-7/2}}$. Assuming coronal heating occurs close to the Sun, it is reasonable to assume a conserved, radially outward heat flux

$$\nabla \cdot \mathbf{F} = -\frac{1}{r^2}\frac{d}{dr}\left(r^2 \kappa_0 T^{5/2} \frac{dT}{dr}\right) = 0. \tag{8.2}$$

outside a boundary at $r = R_\odot$ at a temperature T_0. Assuming also that the temperature profile goes to zero at infinity, (8.2) has the solution

$$T = T_0 \left(\frac{R_\odot}{r}\right)^{2/7}. \tag{8.3}$$

Because of the high conductivity, the temperature profile falls off very slowly with distance; for $T_0 = 10^6\,\mathrm{K}$, the temperature at the orbit of the Earth ($r = 215 R_\odot$) implied by (8.3) is about $2 \times 10^5\,\mathrm{K}$. If the corona is in static equilibrium under pressure and gravity forces, then

$$\frac{dP}{dr} = -\frac{GM_\odot \eta}{r^2}, \tag{8.4}$$

where P is the pressure, η is the mass density of the gas, G is the gravitational constant, and $M_\odot$ is the solar mass. The mass density is given by $\eta \approx n m_p$, where n is the number density of electrons. Assuming a single temperature for electrons and ions, the pressure is $P = 2nk_BT$, where k_B is the Boltzmann constant. Using these relations for the mass density and pressure in equation (8.4) together with (8.2) leads to the solution

$$n = n_0 x^{2/7} \exp\left[\frac{7\lambda_0}{5}\left(\frac{1}{x^{5/7}} - 1\right)\right], \tag{8.5}$$

where $x = r/R_\odot$, n_0 is the number density at $r = R_\odot$, and

$$\lambda_0 = \frac{GM_\odot m_p}{2k_B R_\odot T_0}. \tag{8.6}$$

Equations (8.3) and (8.5) represent the Chapman model for a static corona. The pressure implied by the model is

$$P = P_0 \exp\left[\frac{7\lambda_0}{5}\left(\frac{1}{x^{5/7}} - 1\right)\right], \tag{8.7}$$

where $P_0 = 2n_0 k_B T_0$ is the pressure at the coronal base. The Chapman model has the undesirable characteristic that the pressure is finite at large distances from the Sun, and heads towards the value $P_\infty = P_0 \exp(-7\lambda_0/5)$. For coronal densities and temperatures, $P_\infty \approx 10^{-6}$ Pa. Although conditions in the interstellar medium are not well known, the pressure is thought to be much lower than this, by a factor of 10^7 or so. Hence, the Chapman model cannot merge smoothly with the interstellar medium. At least a strong shock would be required.

Parker realized that this mismatch was not just an artifact of the model but implied that the solar corona could not be in hydrostatic equilibrium out to large distances from the Sun. Motivated also by Biermann's arguments for a continuous, rapid outflow of material from the Sun, Parker began to investigate an alternative solution, a corona in continuous expansion.

Before proceeding I note that the single particle analysis described in the previous Lecture for the origin of the corona, the so-called velocity filtration (or exospheric) model for the corona, implies that coronal particles with sufficient thermal energy should be able to overcome the Sun's gravity. These particles are then free to move out into the interplanetary medium, and with a continuous supply of energy to photosphere would imply a continuous stream of hot particles leaving the Sun. Moreover, considering electrons and protons separately, I noted that electrons would naturally satisfy the energy requirements, thereby setting up an ambipolar electric field that would cause the protons to drift out at the same average speed as the electrons. However, these ideas were not considered in the late 1950s, so Parker's model for the solar wind (although not incompatible) was developed along different lines.

8.2 Parker's solution for an unmagnetised wind

Parker considered the next simplest solution – a spherically symmetric corona in steady motion. The influence of the magnetic field and of rotation are neglected. The time-steady equation of motion for the fluid is then (see Eq. (2.26) in Lecture 2)

$$\eta u \frac{du}{dr} = -\frac{dP}{dr} - \frac{GM_\odot \eta}{r^2}\ , \tag{8.8}$$

where u is the speed of expansion, assumed to be purely radial. The pressure gradient may be eliminated by writing $dP/dr = (dP/d\eta)d\eta/dr$ and using the adiabatic equation of state, which gives $dP/d\eta = \Gamma P/\eta = c_s^2$ (c_s is the adiabatic sound speed). Conservation of the mass flux requires $\eta u r^2 =$ constant, which may be used to eliminate $d\eta/dr$. In this way Eq (8.2) reduces to

$$\frac{(u^2 - c_s^2)}{u}\ \frac{du}{dr} = \frac{2c_s^2}{r} - \frac{GM_\odot}{r^2}\ . \tag{8.9}$$

The nature of solutions to (8.9) is best seen by considering the simple case of an isothermal atmosphere ($\Gamma = 1$), following Parker's original paper. First note that the form of equation (8.9) indicates that it is only possible to have $u = c_s$ at $r = r_c$, where

$$r_c = \frac{GM_\odot}{2c_s^2}. \tag{8.10}$$

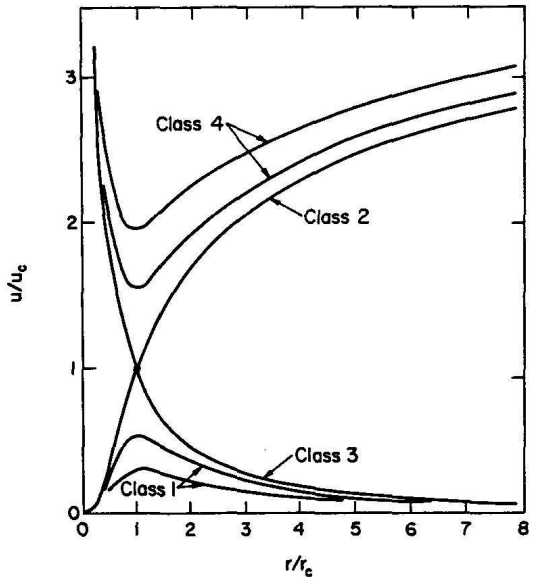

Figure 8.1: Solutions for an isothermal spherical wind [Hundhausen, 1972], with $u_c = c_s$.

At this critical point, the left and right hand sides of (8.9) vanish simultaneously. The advantage of the isothermal case is that (8.9) is integrable, since c_s is constant, and the solution may be written

$$\left(\frac{u}{c_s}\right)^2 - \ln\left(\frac{u}{c_s}\right)^2 = 4\ln\left(\frac{r}{r_c}\right) + \frac{4r_c}{r} \; + \; C, \tag{8.11}$$

where C is the constant of integration. The solutions to (8.11) depend on C, and are illustrated in Figure 8.1 Four classes of solution are labelled in the figure, depending on whether $u(r_c)$ is smaller or larger than c_s. The solutions have different behaviour at small r and as $r \to \infty$, as shown.

Parker chose Class 2 as the solution of physical relevance to the Sun, for the following reasons. For the Sun we require a small speed at $r = R_\odot$, which is true for the solutions of Class 1 and Class 2. For the Sun we also require a small pressure at large r, as explained in the discussion of the Chapman model. For an isothermal wind $P \propto \eta$, and using the mass conservation relationship $\eta r^2 u = \text{const}$, it follows that the pressure at large r will be small provided u is large at large r. This points to solutions of Class 2 or Class 4. Hence only the solution of Class 2 satisfies both requirements. [This solution corresponds to $C = -3$ in Equation (8.11), as may be verified by substituting $u = c_s$ and $r = r_s$.] Parker's solution passes through the critical point (the model places the critical point at about $11.5R_\odot$ for a million-degree corona) and the wind is supersonic for $r > r_c$.

There is a close analogy between the solar wind and a *de Laval nozzle*, which is used to attain supersonic flow in rocket exhausts. The nozzle (illustrated in Figure 8.2) has a varying cross section, $A(z)$, where z is the coordinate along the axis of the nozzle, in the direction of motion of the fluid. The equation of motion for gas in the nozzle (neglecting gravity) is

$$\eta u \frac{du}{dz} = -\frac{dP}{dz} \; . \tag{8.12}$$

Following a similar procedure to that used to derive (8.9) it follows that adiabatic

flow through the nozzle satisfies the differential equation

$$\frac{(u^2 - c_s^2)}{u} \frac{du}{dz} = \frac{c_s^2}{A} \frac{dA}{dz} \ . \tag{8.13}$$

When the flow is subsonic ($u < c_s$), du/dz and dA/dz have opposite signs. Hence a narrowing of the tube will accelerate the flow, as expected from everyday experience with (nearly) incompressible fluids. However, when the flow is supersonic ($u > c_s$), the behaviour is counter-intuitive. Then du/dz and dA/dz have the same sign, so a widening of the tube is required to accelerate the flow. For a flow to continuously accelerate from subsonic to supersonic, it is neccesary to have a structure that narrows and then widens — the de Laval nozzle. The sonic point, $u = c_s$, is achieved at the neck of the nozzle where dA/dz is zero.

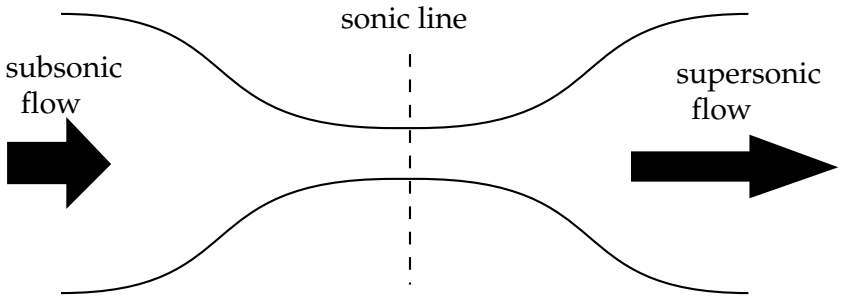

Figure 8.2: At a de Laval nozzle an incoming subsonic flow becomes supersonic.

Comparison of equations (8.9) and (8.13) shows the similarity of the physical systems; the gravitational field in (8.9) effectively plays the role of a nozzle. Note that the r-dependence on the right hand side of (8.9) must be such that the critical point is outside the Sun for a solar wind solution to exist.

Parker's supersonic wind theory was controversial for several years, despite the agreement of the model with the speeds inferred from Biermann's interpretation of comet tails. The controversy was resolved in in favour of Parker's model when the first in situ observations (in the early 1960s) confirmed that the interplanetary region is pervaded by a supersonic flow of solar plasma.

8.3 The magnetized solar wind

The foregoing model for the solar wind neglects magnetic forces. Some rationales for this can be seen by comparing the sizes of the terms in the steady-state MHD momentum equation [e.g., Cravens, 1997]:

$$\eta \mathbf{u}.\nabla \mathbf{u} = -\nabla p + \mathbf{J} \times \mathbf{B} + \eta \mathbf{g} \tag{8.14}$$

$$\eta u^2/L : p/L : B^2/(\mu_0 L) : \eta g \tag{8.15}$$

$$M_A^2 : \beta \approx c_s^2/V_A^2 : 1 : U_{grav}/V_A^2 \ . \tag{8.16}$$

Here L is a characteristic distance in the corona and $U_{grav} = GM_S/R_S$. These terms vary in their characteristic size with position in the corona, as illustrated in Table 8.1. Close to the photosphere and chromosphere it appears legitimate to neglect magnetic field effects - at larger radial distances it is not. This Section considers the effects of the magnetic field, first kinematically using the frozen-in assumption and then dynamically.

Location	r/R_S	M_A^2	β	U_{grav}/V_A^2
photosphere	1.01	10^{-3}	10	10
chromosphere	1.04	10^{-3}	0.5	0.5
corona	3	0.3	0.1	0.1
corona	10	1	0.05	0.05

Table 8.1: Characteristic sizes of terms in the MHD momentum equation (8.16) from the photosphere to the corona, after Cravens [1997].

8.3.1 The Parker spiral model for the magnetic field

Parker also considered the implication of the solar wind in regard to the configuration of the Sun's magnetic field. The high electrical conductivity of the plasma means that the field is frozen-in to the plasma (see Lecture 2). The magnetic field must therefore be transported out into interplanetary space by the wind. The shape of the magnetic field lines is then determined by the wind velocity together with the rotation of the Sun.

If the wind is purely radial (i.e. $\mathbf{u}$ has only the component $u_r = u$), then in a spherical coordinate system rotating with the Sun, the solar wind velocity has components

$$U_r = u, \quad U_\phi = -\Omega_\odot r \sin\theta, \quad U_\theta = 0, \tag{8.17}$$

where $\Omega_\odot = 2.7 \times 10^{-6}\,\mathrm{rad\,s^{-1}}$ is the angular velocity of the Sun's rotation (differential rotation is neglected in this simple treatment). The nonradial velocity component is due to the transformation to the rotating frame. The path followed by the magnetic field is a velocity streamline in this rotating frame and so is defined by

$$\frac{1}{r}\,\frac{dr}{d\phi} \;=\; \frac{U_r}{U_\phi} \;=\; -\frac{u}{\Omega_\odot r \sin\theta}\;. \tag{8.18}$$

The Parker solution predicts that for distances several times larger than r_c, the wind speed u is almost constant. Assuming $u = u_0$ (a constant), then (8.18) can be integrated to give

$$r - R_\odot = -\frac{u_0}{\Omega_\odot \sin\theta}(\phi(r) - \phi_\odot), \tag{8.19}$$

where $\phi_\odot$ is the initial azimuthal angle at the surface of the Sun. Equation (8.19) describes a geometrical figure known as an Archimedean spiral. The *winding distance*, ΔR, is the radial distance in which the spiral has wrapped once around the Sun. From (8.19), $\Delta R = 2\pi u_0/\Omega_\odot$. For a wind speed $u_0 = 400\,\mathrm{km\,s^{-1}}$, $\Delta R \approx 6\,\mathrm{AU}$.

Figure 8.3 shows a dramatic confirmation of the Parker spiral achieved via tomographic inversion of radio scintillation measurements.

Similar direct evidence for the Parker spiral is shown in Figure 4.8 of Lecture 4 on plasma waves, based on triangulation of the source locations of electron beams generating type III solar radio bursts while propagating away from the Sun into the solar wind.

The idea that the fluid flow moves strictly radially whilst the streamlines of the flow are curved may be understood by reference to a phonograph player, where the needle moves only radially whilst tracing the spiralling grooves of a record. Figure 8.4 illustrates the motions involved. It should also be noted that whilst the geometrical figure of the fieldlines co-rotates, the fluid accelerated by the solar wind does not co-rotate but instead moves radially outwards. In contrast, material on closed field lines in the solar corona must co-rotate.

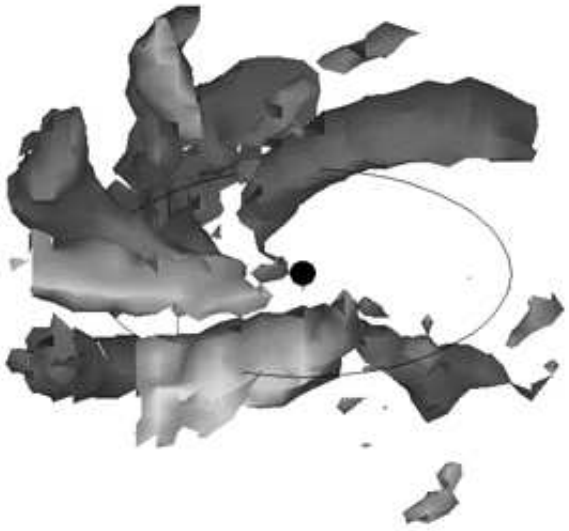

Figure 8.3: A 3-D reconstruction of the heliospheric plasma, based on radio scintillation measurements made from Earth's orbit (the circle). The Parker spiral is clearly visible in the form of the density-enhanced regions. [http://www.sdsc.edu:80/GatherScatter/GSfall96/jackson.html.]

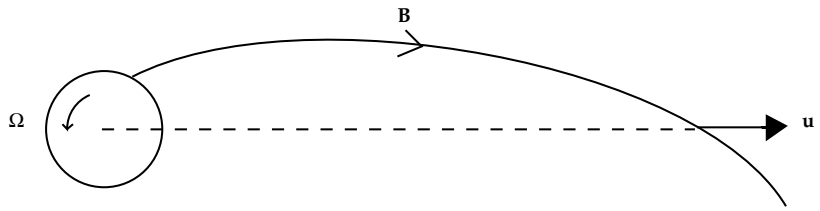

Figure 8.4: The drawing out of a magnetic field line by the solar wind, with radial velocity **u**, is illustrated schematically.

8.3.2 Equatorial magnetized wind models

Parker's treatment of rotation and of the magnetic field is not self-consistent, as illustrated in Table 8.1. The theory was modified to include a magnetic field in a consistent manner about a decade after Parker's initial 1958 work.

The starting points for the theory of a magnetized wind are conservation of mass, the divergence equation for the magnetic field, the frozen-in magnetic field equation, and the momentum equation. The rate at which the Sun loses mass is constant in a steady-state model, and is given by

$$\dot{M} = 4\pi\eta r^2 u_r \ . \tag{8.20}$$

This equation then show that $\eta \propto r^{-2}$ in regions where u_r is constant. Such regions are often called "wind-like" regions.

Conservation of magnetic flux in the wind ($\nabla\cdot\mathbf{B} = 0$) leads to

$$B_r r^2 = B_{r\odot} R_\odot^2, \tag{8.21}$$

with the assumptions that $B_\theta = 0$ and that B_ϕ is constant, either for all ϕ or in small regions (flux tubes) in which the derivative $\partial B_\phi/\partial\phi$ can be neglected.

For simplicity now, the fluid velocity and magnetic field are assumed only to have radial and azimuthal components in spherical coordinates, $\mathbf{u} = u_r\hat{\mathbf{r}} + u_\phi\hat{\boldsymbol{\phi}}$ and $\mathbf{B} = B_r\hat{\mathbf{r}} + B_\phi\hat{\boldsymbol{\phi}}$. This restricts the description to equatorial magnetized winds.

The next equation for a magnetized wind is provided by the frozen-in field condition ($\mathbf{E} = -\mathbf{u}\times\mathbf{B}$) which with $\nabla\times\mathbf{E} = 0$ for a static magnetic field ($\partial\mathbf{B}/\partial t = 0$) implies

$$\nabla\times(\mathbf{u}\times\mathbf{B}) = 0. \tag{8.22}$$

This leads to three vector equations, of which the θ component leads to nothing useful. The ϕ-component of (8.22) requires

$$\frac{\partial}{\partial r} r(u_\phi B_r - u_r B_\phi) = 0\ . \tag{8.23}$$

The r component leads to

$$\frac{\partial}{\partial \phi} r(u_\phi B_r - u_r B_\phi) = 0. \tag{8.24}$$

On integrating (8.23), the constant of integration is found by considering the boundary condition at $r = R_\odot$.

$$B_\phi = \frac{u_\phi B_r + C}{r u_r}\ . \tag{8.25}$$

Using the flux conservation condition (8.21) leads to

$$B_\phi = \frac{B_\phi(R_\odot)R_\odot}{r} - B_r\frac{\Omega_\odot(r - R_\odot)}{u_r}\ . \tag{8.26}$$

. Usually the magnetic field is assumed to be radial at the source surface, idealized here as occurring at $r = R_\odot$, so that $B_\phi(R_\odot = 0$, and is is assumed that u_r is constant. The magnetic field can then be shown to lie on spiral shapes, consistent with the foregoing kinetmatic analysis.

A magnetized wind solution is found by integrating the radial component of the equation of motion,

$$\eta\left(u_r\frac{du_r}{dr} - \frac{u_\phi^2}{r}\right) = -\frac{dP}{dr} - \frac{B_\phi}{\mu_0 r}\frac{d}{dr}(rB_\phi) - \frac{GM_\odot\eta}{r^2}\ . \tag{8.27}$$

There is only one solution that has $u_r = 0$ at the surface of the star and that is supersonic at large distances. Figure 8.5 illustrates the solutions to (8.27) and the physically acceptable solution (the central solid line). There are three critical points in the magnetized case, and the physically acceptable wind solution passes through all of them. Near the Earth, the flow speed of the solar wind is known to be superalfvénic. The Alfvén radius, r_A, where the flow speed passes through the Alfvén speed, is thought to occur at $r_A = 10$–$20R_\odot$.

From (8.21), the radial component of the field falls off according to $B_r \propto r^{-2}$. The variation of the azimuthal field may be determined from (8.25); at large distances, u_r is almost constant, and so the dominant variation is $B_\phi \propto r^{-1}$. Hence the field spirals tighten with increasing distance from the Sun, becoming almost circular. This property was also apparent in the simple unmagnetized treatment due to Parker, presented in Section 8.2 via Eq. (8.18).

We now turn to another topic, which is really an aside on the rate of angular momentum loss from the Sun. Returning to Eqs (8.20) and (8.21), they imply that

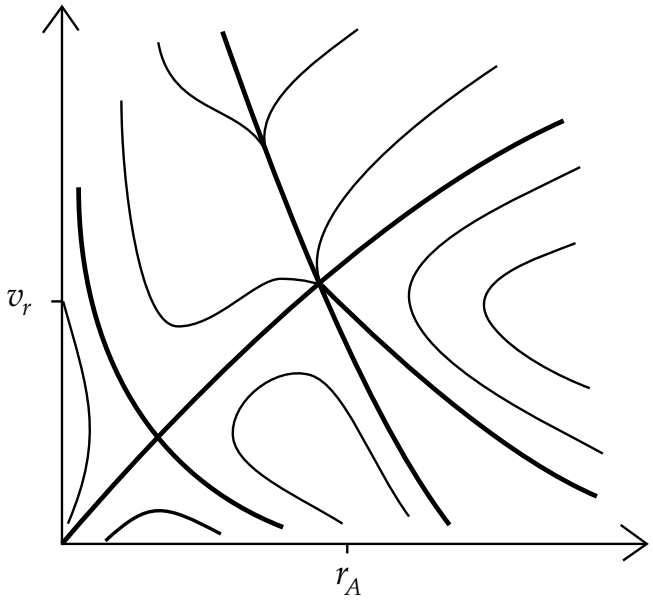

Figure 8.5: A schematic showing solutions to Eq. (8.27). There are three critical points, corresponding to the flow speed being equal to the speed of the slow, Alfvén and fast modes, but the latter two are so close together that they are indistinguishable in the figure. The only acceptable solution is the central solid curve that passes through all three critical points and gives a supersonic flow at infinity.

$\eta u_r/B_r = \dot{M}/4\pi B_\odot R_\odot^2$ is a constant. Hence Eq. (8.23) may be integrated trivially, giving

$$r\left(u_\phi - \frac{B_r B_\phi}{\mu_0 \eta u_r}\right) = \ell, \tag{8.28}$$

where the constant of integration, ℓ, may be interpreted as the angular momentum per unit mass. Now Eqs (8.28) and (8.25) may be rewritten in the form

$$r u_\phi = \frac{M_A^2 \ell - \Omega_\odot r^2}{M_A^2 - 1}, \tag{8.29}$$

where

$$M_A^2 = \frac{u_r^2}{B_r^2/(\mu_0 \eta)} \tag{8.30}$$

is the radial Mach number.

The Alfvénic critical point is defined as the point at which the radial flow is equal to the Alfvén speed, that is, $M_A = 1$. Now u_ϕ must remain finite everywhere, and hence the numerator in (8.29) must vanish at the point where M_A passes through unity. Let the Alfvénic critical point be at $r = r_A$, with $M_A = 1$ there by definition. The vanishing of the numerator in (8.29) at this critical point gives $\ell = \Omega_\odot r_A^2$, and thus determines the angular momentum per unit mass at $r = r_A$. The angular momentum loss rate is then $\dot{M}\ell = \dot{M}\Omega_\odot r_A^2$. Thus (8.29) implies that, from the viewpoint of the amount of angular momentum carried off, the plasma is effectively thrown off with a lever-arm of length r_A. Specifically, the angular momentum carried off by the rotating, magnetized solar wind is equivalent to that implied by rigid rotation out to the Alfvén radius r_A.

The Sun is thought to have been rapidly rotating when it first formed, and to have lost most of its angular momentum to the solar wind. To understand this effect

of the magnetized wind, suppose that the solar wind were unmagnetized. Then it would carry off angular momentum at the rate $\dot{M}\Omega_\odot R_\odot^2$, which is determined by the angular momentum per unit mass of the wind as it leaves the solar surface. For the actual value of $\dot{M}$, this rate is too small to lead to any significant reduction of the angular momentum of the Sun over its life time. Now consider a magnetized wind, for which the angular momentum loss rate is $\dot{M}\Omega_\odot r_A^2$. This is larger than that for an unmagnetized wind by the factor $r_A^2/R_\odot^2 \sim 10^2$–$10^3$, and is large enough to have slowed down the Sun significantly in its life time. The Sun appears to have lost nearly all its angular momentum to its wind (nearly all the angular momentum of the solar system is in the planetary motions, overwhelmingly dominated by Jupiter's contribution).

8.4 The fast and slow solar wind

In situ observations at 1 AU have established that there are two components to the quiescent solar wind, viz. high-speed streams ($u \approx 700\,\mathrm{km\,s^{-1}}$), and low-speed streams ($u \approx 350\,\mathrm{km\,s^{-1}}$). There are also transient flows (coronal mass ejections, or CMEs) that can be faster again, but the discussion of these is deferred to Lecture 9. The low-speed wind is denser than the high speed wind ($n \approx 10^7\,\mathrm{m^{-3}}$ as opposed to $n \approx 3 \times 10^6\,\mathrm{m^{-3}}$), and carries a greater flux of particles. The high-speed wind originates in coronal holes, whereas the low-speed wind comes from dense coronal streamers straddling magnetic neutral lines at the Sun, which tend to be either equatorial (near solar minimum) or else lie along the streamer belts at intermediate latitudes.

The Ulysses mission is an out-of-the-ecliptic spacecraft that has provided detailed information on the latitudinal structure of the solar wind. Ulysses used a Jupiter swingby in February 1992 to take it on an orbit that passed over the south pole of the Sun for the first time in September 1994, and over the north pole in July 1995. The second pass over the poles was in 2000/2001, close to solar maximum. Figure 8.6 illustrates Ulysses measurements of the solar wind speed versus latitudes for the two passes, and the relationship of the wind speed with the inner coronal structure. Ulysses found the polar solar wind to be a very uniform, high-speed flow, and has provided a wealth of detail on the three-dimensional structure of the magnetic field in the solar wind, on the interactions between low- and high-speed streams, and on transient disturbances in the wind.

The high-speed wind is difficult to explain in the context of theoretical models of the type discussed above. Thermally driven winds do not attain such high speeds, and it is necessary to provide additional energy and momentum to the wind at $\geq 15R_\odot$ to reproduce the observations (e.g. Withbroe 1988). One popular model involves the ad hoc assumption of a flux of Alfvén waves that dissipates in the wind. The in situ detection of Alfvénic fluctuations at 1 AU provides some support for this model.

High-speed streams in the solar wind tend to be unipolar, i.e. the magnetic field within the flow points either entirely away from or entirely towards the Sun along the archimedean spiral. The magnetic polarity of a stream is determined by the polarity of the coronal hole from which the stream originates. Field polarity reversals occur within slow-speed streams, and these reversals correspond to crossings of the heliospheric current sheet (HCS) that encircles the Sun. If the (approximately) dipole global field of the Sun is inclined, the rotation of the Sun leads to the HCS having a "ballerina's skirt" configuration. The interaction of low- and high-speed streams can lead to the formation of shocks in the wind.

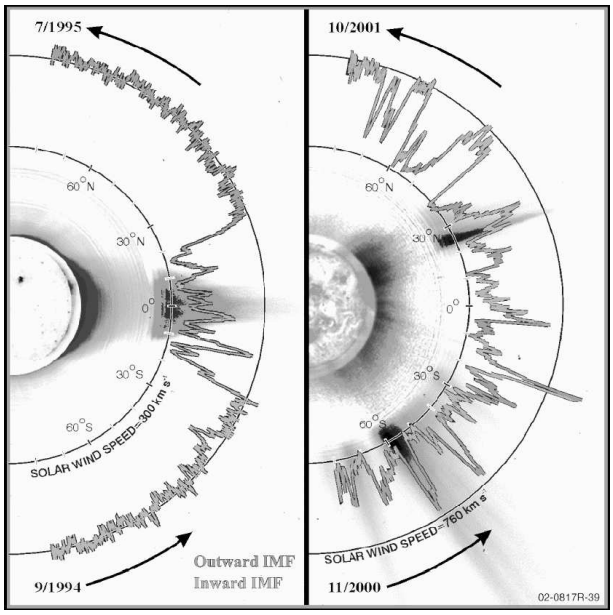

Figure 8.6: Ulysses observations of the speed of the solar wind as a function of latitude, overlayed on an image of the structure of the corona during the period of observation. From D. McComas and colleagues at http://solarprobe.gsfc.nasa.gov/solarprobe_science.htm.)

References

This lecture is based in part on earlier lecture by D.B. Melrose and M. Wheatland, the latter based in part on an outline written by I.H. Cairns. Additional references are:

Cravens, J. 1997, *Physics of Solar System Plasmas*, Cambridge.

Gosling, J.T. 1996, Annual reviews of Astronomy and Astrophysics, **34**, 35

Hundhausen, A.J. 1972, *Coronal Expansion and Solar Wind*, Springer-Verlag, New York

Withbroe, G.L. 1988, Astrophysical Journal **325**, 442